Advances in Materials
2016; 5(5): 51-56
http://www.sciencepublishinggroup.com/j/am
doi: 10.11648/j.am.20160505.14
ISSN: 2327-2503 (Print); ISSN: 2327-252X (Online)

Effect of Sulfur on the Structure and Physical Properties of Vanadium-Iron-Lithium-Silicate Glass and Glass-Ceramics Nano Composite

M. Y. Hassaan[1], H. H. El-Bahnasawy[1], S. M. Salem[1], T. Z. Amer[2], M. G. Moustafa[1], A. G. Mostafa[1]

[1]Phys. Department, Faculty of Science, Al-Azhar University, Nasr City, Cairo, Egypt

[2]Phys. Department, Faculty of Science, Al-Azhar University, (Girls Branch) Nasr City, Cairo, Egypt

Email address:
htagma@hotmail.com (T. Z. Amer)

To cite this article:
M. Y. Hassaan, H. H. El-Bahnasawy, S. M. Salem,T. Z. Amer, M.G. Moustafa, A.G. Mostafa. Effect of Sulfur on the Structure and Physical Properties of Vanadium-Iron-Lithium-Silicate Glass and Glass-Ceramics Nano Composite. *Advances in Materials.* Vol. 5, No. 5, 2016, pp. 51-56. doi: 10.11648/j.am.20160505.14

Received: September 7, 2016; **Accepted**: September 21, 2016; **Published**: October 11, 2016

Abstract: Glass sample with the composition 1 Li_2O • 0.25 Fe_2O_3• 0.25 V_2O_5• 1.5 SiO_2 has been studied for the usage as a cathode material in solid batteries. Another sample with the previous composition in addition to 5wt. % sulfur as reduced agent to yelled multi-valance Fe and V ions was also studied. Both sulfur-free and sulfur-doped glass samples were subjected to heat treatment for one hour at 550°C to obtain two glass–ceramic samples. Structural studies were made using X-ray diffraction (XRD), Mössbauer effect (ME) and Fourier-transform infrared spectroscopy (FT-IR). The precipitation of various phases in heat treated glass samples with particle size in the nano-range was observed in X-ray pattern. Mössbauer spectra indicated that iron exist as a ferric ions occupy two non-equivalent tetrahedral sites in the sulfur-free samples, while ferrous ions in octahedral site in addition to the previous two ferric phases was appeared in sulfur-doped samples. Differential thermal analysis (DTA) was also carried out to monitor the crystallization temperature and the thermal stability of the obtained glasses. DC electrical conductivity measurements exhibit an enhancement of the conductivity of sulfur-doped glass sample compared with sulfur-free which make it more suitable to use as cathode in the solid batteries.

Keywords: Lithium-Silicate Glasses, Glass-Ceramics, Sulfur Doped Glasses, Solid Batteries, Glass Cathode, Mössbauer Spectroscopy, X-ray Diffraction, Fourier-Transform Infrared, DC Electrical Conductivity

1. Introduction

Lithium silicate glasses were considered as excellent materials for integrated optics, photonic and bio-medical applications due to their high thermo-physical, chemical and mechanical stability [1–4]. The addition of transition metal ions (TMIs) like iron and vanadium to the stable lithium silicate glasses is expected to improve their electrical and dielectric features [5-7]. In the last few decades, many articles have been published dealing with the properties and structure of various lithium silicate glasses [8, 9]. The effect of adding sulfur (as reducing agent) on the physical properties and valence state of TMIs of the various glasses has been also reported [10, 11]. Hassaan et al studied the effect of sulfur addition and heat treatment on electrical conductivity of barium vanadate glasses containing iron [10], while El-Desoky et. al studied the effect of adding sulfur on the transport properties of some semiconducting iron phosphate glasses [11]. Moreover, Hassaan et. al concluded that, sulfur can be introduced into glass batches to control the oxidation states of the TMIs, and to enhance the electrical conduction in some lithium nickel silicate glasses and the corresponding glass-ceramics [12].

In the present work, the effect of introducing sulfur and heat treatment on the structure and redox state of the present TMIs as well as the electrical properties of lithium-iron-vanadium-silicate glass has been thoroughly investigated.

2. Experimental

2.1. Samples Preparation

Two glass batches having the molecular composition

$1Li_2O \bullet 0.25\ Fe_2O_3 \bullet 0.25\ V_2O_5 \bullet 1.5\ SiO_2$, were weighted, where in the first batch, 5 wt% sulfur has been introduced, while the second batch was left sulfur-free. Both batches were melted at 1350°C in an electric muffle furnace in air using platinum crucibles for one hour, then they were quenched onto a copper plate at room temperature (RT), to yield two glass samples, sulfur-doped glass sample (SG-sample) and sulfur free glass sample (G-sample) in the form of pellets of 1mm thickness. A part of both samples was heat treated for one hour, at 550°C which is close to their crystallization temperature, as drown from DTA, to obtain two glass-ceramic (heat treated sulfur free glass GC- sample and heat treated sulfur doped glass SGC-sample).

2.2. Samples Characterization

The DTA thermo-gram of the G-sample was obtained using Shimadzu Thermal Analyzer (model DTA 50). The measurement was performed by heating 25 mg powder glass at a fixed heating rate of 10 C°/min using constant amount of Al_2O_3 as reference material in the temperature range (0 - 800°C).

XRD patterns of the studied glass samples and their corresponding glass-ceramics were obtained using [Rigaku RINT 2100, with Cukα, λ= 0.1541 nm]. The maximum current and voltage were 30 mA and 50 kV respectively.

A conventional constant acceleration ME spectrometer out fitted with 10 mCi ^{57}Co radio-active source in rhodium matrix was utilized to obtained the ME spectra at RT. The calibration was performed relative to ME spectrum of a metallic iron foil, while the measured spectra were analyzed using a computer program based on Voigt line shape.

The FT-IR spectra for all the samples were recorded at RT by standard KBr pellet technique using computerized FT-IR spectrophotometer [JASCO FT-IR-300E] in the range (400 – 4000 cm^{-1}).

DC electrical conductivity for all samples was measured by means of the two-probe method, which is appropriate for high resistance materials. Silver painted electrodes were pasted on the polished surfaces of the samples and then situated between two polished and cleaned copper electrodes. KEITHLEY 485 Auto ranging Pico Ammeter was used to collect the DC data over the temperature range (300-550°C). The sample temperature was measured by a chromal–alumal type K thermocouple which is placed as close as possible to the sample.

3. Results and Discussion

3.1. Differential Thermal Analysis

The DTA technique has been utilized here to obtain both the glass transition (T_g) and crystallization (T_c) temperatures of the prepared sulfur-free glass sample. These two characteristic temperatures are usually needed to calculate the thermal stability of amorphous materials and glasses [13]. Also, the value of T_c can be taken as a guide to select the suitable heat treatment temperature for both glasses samples.

Fig. (1) Shows the obtain DTA thermo-gram of the sulfur-free glass sample. This thermo-gram exhibits an endothermic minima which represents the glass transition temperature (T_g), followed by an exothermic peak corresponds to the crystallization temperature (T_c). Also, the appearance of Tg in such thermo-gram can be taken as evidence for the amorphous nature and the randomness character of amorphous solids and glasses. The measured Tg and Tc for such sample is then determined to be 480 and 585°C respectively.

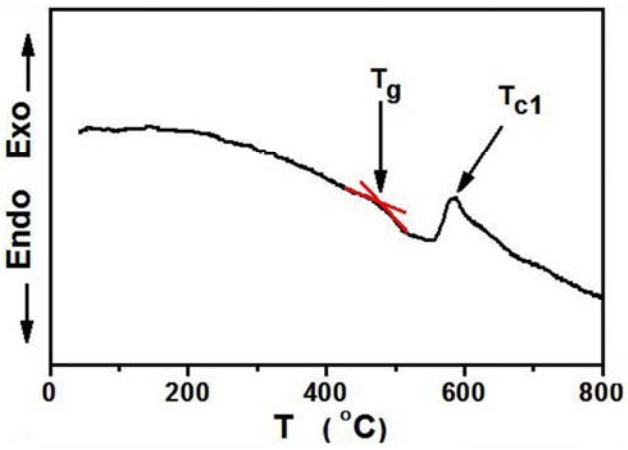

Fig. 1. *The obtained DTA thermo-gram of the sulfur-free glass (G-sample).*

The difference between T_c and T_g was calculated to be 105°C, which is a large value revealing the high thermal stability of the studied glasses. Therefore, it is supposed that lithium-silicate glasses have a lot of modern applications due to their high thermal stability.

According to the obtained value of T_c (585°C) and since the heat treatment temperature must be close to T_c, therefore the heat treatment temperature was selected to be 550°C.

3.2. XRD

XRD patterns of glass G-sample and glass-ceramic samples (GC, SGC) are shown in Fig. (2). A broad hump around 2θ = 25 with no indication of diffraction peaks in the G-sample was found which confirms the amorphous nature for such sample, while the sulfur-doped glass (SG-sample) exhibits similar pattern to this one. The heat treated (HT) samples showed some sharp peaks which identified as LiV (Si_2O_6) (JCPDS card 87–0410) and Li_2 (VO) (SiO_4) crystals (JCPDS card 87–0525) with a structure close to monoclinic.

The obtained XRD data were then used to calculate the average crystallite size as well as the internal micro-strain of the HT samples, using Williamson–Hall (W-H) plot [between β cos (θ) and sin (θ)], applying (W-H) equation [14]:

$$\beta \cos\theta = \frac{c\lambda}{D_{ave}} + 4\varepsilon \sin\theta$$

Where β is the full width at half maximum (FWHM), θ is the Bragg angle, C is the correction factor ($c \approx 1$), D_{ave} is

the average crystallite size, λ is the wave length of the used X-ray, ε is the lattice micro-strain. Such plots are shown in Fig. (3), for the GC and SGC samples respectively. The obtained values are then listed in Table (1).

From Table (1), the average crystallite size of the SGC sample is greater than that of GC, but all are in the nano-size range.

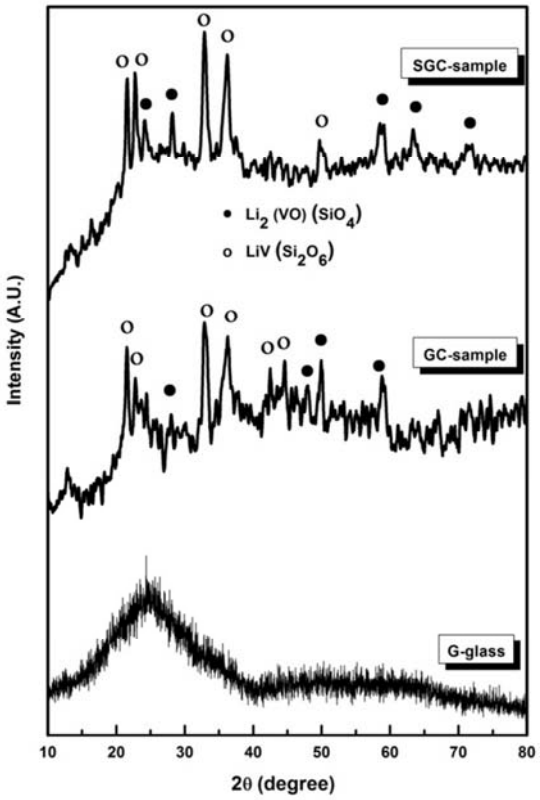

Fig. 2. *XRD of sulfur free glass G-sample and glass-ceramic with samples.*

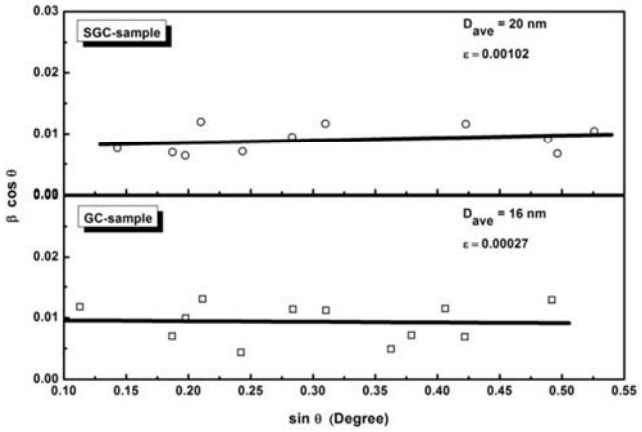

Fig. 3. *W-H plot for the GC and SGC samples.*

Table 1. *The calculated values of crystallite size and internal micro-strain.*

Sample	Crystallite size nm	Micro-strain
GC	16	0.00027
SGC	20	0.00102

3.3. Mössbauer Spectroscopy

Room temperature Mössbauer spectra (MS) of the different samples are shown in Fig. (4). A computer program based on Voigt profile - which is more convenient for such like amorphous materials - is used to analyze and extract the hyperfine Mössbauer parameters from the above spectra. The line width of centered Lorentzian profile was fixed at 0.25 mm/s while the widths of Gaussian distribution (GW) are listed in Table (2). Phases assignment of the obtain Mössbauer parameters (isomer shift, IS mm/s and quadrupled splitting, QS mm/s) have been made according to several authors [15, 16]. As shown in Table (2), the data indicate the presence of two Fe^{3+} phases (I, II) in the sulfur-free glass sample which characterized as Fe^{3+} ions in two nonequivalent tetrahedral sites, where phase II may be due to Fe^{3+} ions occupying a highly distorted tetrahedral site than that of phase I, which means that is the iron ions in both these states (I & II) occupy the glass network former positions. After sulfur addition, the above two phases appeared in addition to a weak doublet characterizing Fe^{2+} ions in octahedral site, phase (III), acting as glass network modifier. The reduction effect resulting from adding sulfur was essentially aiming to forming this Fe^{2+} phase.

From the area ratios of the different phases, it can be seen that the amount of the reduced iron ions in the sulfur-doped samples was formed at the expense of phase II that is the highly distorted ferric ions. Also, the values of QS and GW due to phase II indicated that the addition of sulfur yielded a more disordered glass network.

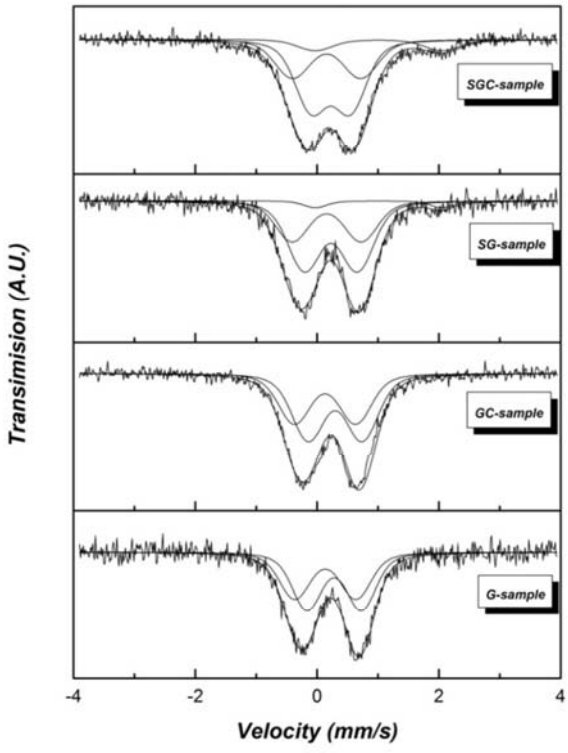

Fig. 4. *Room temperature Mössbauer spectra of the studied samples.*

Table 2. *The calculated ME hyperfine parameters of all the studied samples.*

	Fe^{3+} tetrahedral site (I)				Fe^{3+} highly distorted tetrahedral site (II)				Fe^{2+} octahedral site (III)			
	IS (mm/s)	QS (mm/s)	GW (mm/s)	Area%	IS (mm/s)	QS (mm/s)	GW (mm/s)	Area%	IS (mm/s)	QS (mm/s)	GW (mm/s)	Area%
G	0.280	0.879	0.182	55.7	0.135	1.011	0.191	44.3	-	-	-	-
GC	0.297	0.890	0.209	56.8	0.131	1.002	0.205	43.2	-	-	-	-
SG	0.223	0.878	0.186	58.1	0.157	1.371	0.237	34.7	1.01	2.077	0.129	7.3
SGC	0.225	0.644	0.207	59.1	0.154	1.125	0.230	31.7	1.02	2.083	0.237	9.2

The slight increase in the amount of ferrous ions in the spectrum of the sulfur-doped glass-ceramic (SGC-sample) than that of the sulfur-doped glass (SG-sample) may be due to the effect of HT. The effect of heat treatment on the glass samples was less pronounced in the ME than that in XRD.

3.4. Fourier-Transform Infrared Spectroscopy

The obtained IR absorption spectra of the studied samples are shown in Fig (5). Similarities can be observed between the spectra of both glass samples which differ from those of the glass-ceramics. The major feature of the spectra of glasses is the broadening of absorption bands while a remarkable splitting in some bands of the glass-ceramics is observed.

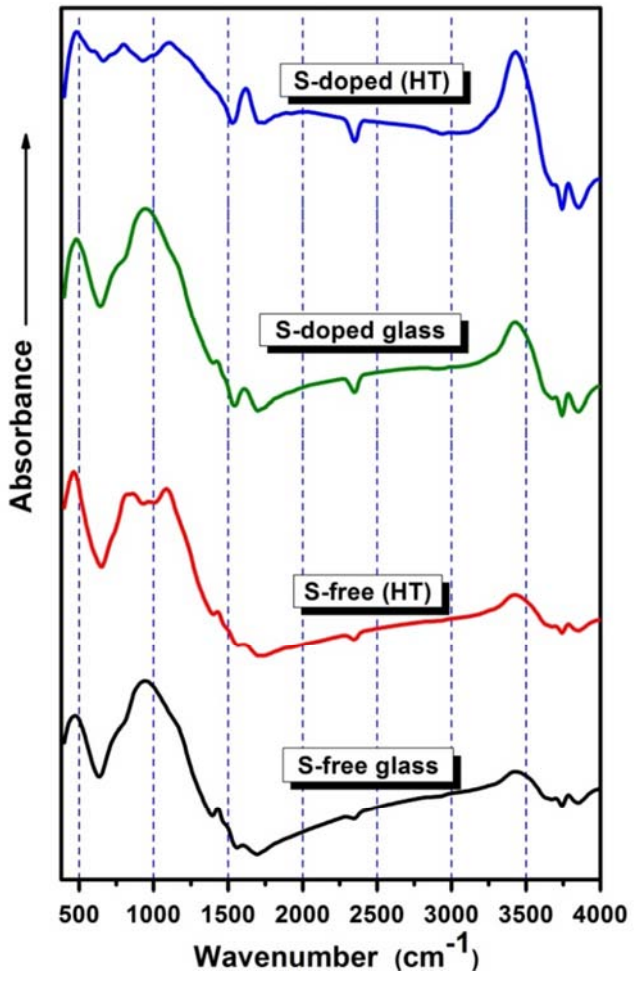

Fig. 5. *FTIR absorption spectra of the studied samples.*

Inspecting all the obtained spectra, it can be state that:

a A band at about 480 cm^{-1}, in all spectra (glasses and glass-ceramics) shows a slight broadening in the glass samples. Most probable it is a resultant of two overlapped bands. The first can be attributed to Si–O–Si bending vibration in SiO_4 tetrahedral groups [17, 18], while the second one may be due to the presence of some V–O–V linkages between vanadate layers and chains [19]. In the spectra of both glass-ceramic samples, this band may hide a very small one that due to some iron ions occupy FeO_6 groups acting as glass network modifier [20].

b A slight band appeared in the spectrum of the SGC sample at about 650 cm^{-1}while it appeared as a slight shoulder in the rest spectra. Such band can be attributed to the presence of ferric ions in the tetrahedral coordination symmetry acting as network former [21].

c A shoulder band appeared at about 710 cm^{-1} in all spectra, but in the spectrum of the SGC, it appeared as a single one. This band can be attributed to symmetric stretching vibrations of Si–O–Si bridging bonds [22] as well as to the stretching vibrations of V–O–V [23] in addition to some S–O–S stretching vibration [24].

d A broad band appeared at about 940 cm^{-1} in the spectra of glasses only (sulfur-free and sulfur-doped), where it de-convoluted into two different bands in the spectra of the glass-ceramic samples to be at 870 and 1080 cm^{-1}. These bands can be attributed to some asymmetric stretching vibrations of Si–O–Si bridging bonds [22] and V═O (double bond) in tetragonal VO_4 groups [21] as well as some Fe–O–S bridging bond [24].

e The band that appeared at 1430 cm^{-1} is assigned to some deformed vibration of H–O–H groups diffused throw the structure of glass or surface adsorbed water [25].

f The band at 1600 cm^{-1} is due also to the deformed vibration modes of H_2O groups [26, 27].

g Besides, the bands appeared around the region 3430 $cm^{-1}$is due to the stretching vibration modes of some O–H and H–O–H groups as well as the vibration of some hydrogen bonds [14, 27]. The presence of some H_2O and OH groups may be due to the applied KBr disk technique.

Based on the obtained IR results it can be supposed that various deformed silicate groups are easily detected since SiO_2 represents the main glass former. Some bond vibrations due to both vanadium and iron are observed since they act mainly as glass network also. It can be also supposed that

some bond vibrations appeared as a result the formation of S–O–S bonds and some Fe–O–S bonds in the glass network.

3.5. DC Electrical Conductivity

Electrical properties of oxide glasses containing transition metal ions are improved due to the presence of such ions in more than single valence state. The conductivity in this case is described by electron hopping between the present various ionic states [28, 29]. However, the DC electrical conductivity of the studied samples was measured in the temperature range from 300 to 550°C. The electrical conductivity of all the studied samples was investigated in an Arrhenius plot, Fig. (6).

The approximately straight lines obtained in the Arrhenius plot allow expressing the apparent conductivity as a function of temperature according to the relationship:

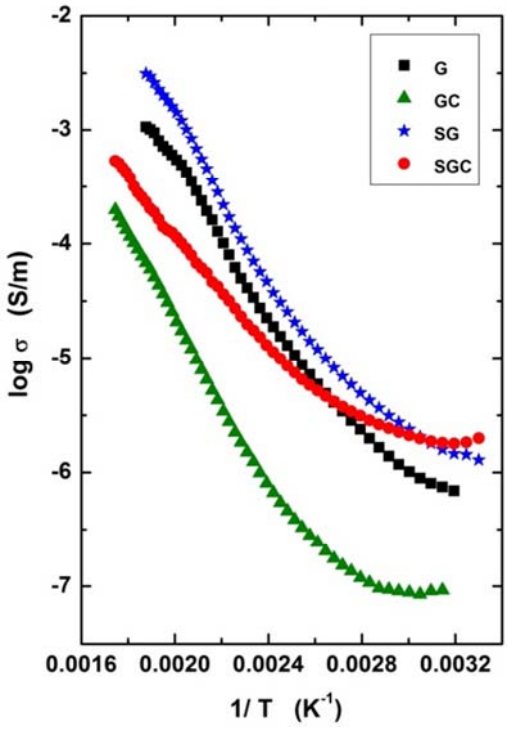

Fig. 6. *The electrical conductivity of all the investigated samples.*

$$\sigma = \sigma_o \, exp\,[-W_{dc}/K_B T]$$

Where σ_o is the pre-exponential factor, W_{dc} is the activation energy, T is the absolute temperature and k_B is Boltzmann constant.

The activation energy for the thermally activation hopping process was obtained by fitting the linear part of the conductivity data with Arrhenius equation. Values of W_{dc} and σ obtained at 463°C are listed in Table (3).

However, Fig (7), exhibits a comparison between the values of log (σ) at 463°C for all the studied samples. From this figure, it is observed that the sulfur-doped glass exhibits the highest conductivity and the lowest activation energy than all other samples. This is due to the supposition that the addition of sulfur acts to reduce some ferric ions to appear as ferrous ions, which in turn adding a new contribution to the conduction process through the hoping mechanism. The presence of these ions (ferric and ferrous) was confirmed by ME and IR results [30].

Table 3. *W_{dc} and log (σ) values at 463°C for the studied samples.*

Sample	Log (σ) at 463°C (S/m)	W_{dc} (eV)
G	-3.79	0.32
GC	-5.28	0.35
SG	-3.45	0.27
SGC	-4.51	0.29

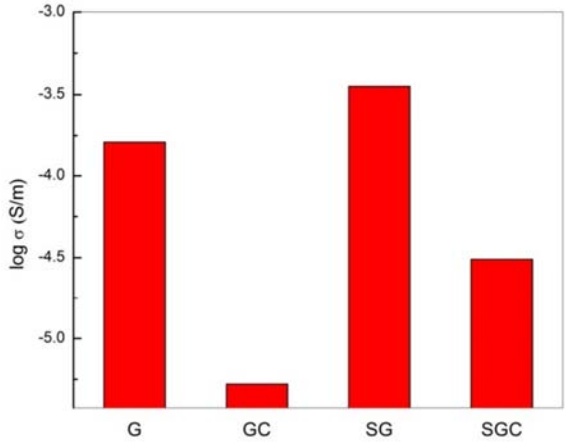

Fig. 7. *Comparison between the values of log (σ) at 463°C for the studied samples.*

On the other hand, the observed decrease of the electrical activation energy in case of glasses than the corresponding glass-ceramic samples and hence increasing the electrical conductivity is attributed to the randomly dispersed nanocrystallites which produce an ion-blocking effect imposed only on lithium ions which act to prevent the ionic conductivity in the HT samples. These results are found in good agreement with other previous work [12, 31]. The higher conductivity of the SGC than that of GC - despite the former has lager average crystallite size - can be attributed to the higher presence of 9.2% from the total iron as Fe^{2+}.

4. Conclusion

According to the obtained results, it can be concluded that:

a The studied glasses are thermally stable, where their $[T_c\text{-}T_g] = 105°C$.

b XRD patterns confirmed the amorphous nature of the studied glasses, also it indicated that [LiV (Si_2O_6)] and [Li_2 (VO) SiO4] are the main crystals precipitated during HT.

c The crystallite volume was found to be 20 and 16 nm, while the internal micro-strain was found to be 0.00102 and 0.00027 for sulfur-free and sulfur-doped HT samples respectively.

d ME measurements, it indicated that only Fe^{3+} in the tetrahedral coordination symmetry acting as glass-network former in the sulfur-free glass and glass-ceramic (G & GC). While in the sulfur-doped glass and

glass-ceramic (SG & SGC), most iron ions occupy Fe^{3+} in the tetrahedral coordination symmetry is acting as glass-network former (from 90.8% to 92.8%), in addition to a little Fe^{2+} in the octahedral coordination symmetry acting as glass network modifier (from 9.2% to 7.2%).

e IR analysis indicated the appearance of different silicate groups and various bond vibrations due to vanadium and iron.

f The sulfur-doped glass sample exhibits the higher conductivity and the lower activation energy than other samples, due to the presence of both Fe^{2+} and Fe^{3+}, as well as the high mobility of lithium ions.

g Both the glass-ceramic samples exhibit less conductivity than the corresponding glasses due to the blocking effect of lithium ions in the HT matrix.

h The enhancement of conductivity in sulfur-doped glass sample make it more convenient to use as a cathode material in solid batteries compared to other samples.

References

[1] A. O. G. Dikovska, P. A. Atanasov, M. Jiménez de Castro, A. Perea, J. Gonzalo, C. N. Afonso & J. GarcíaLópez, Thin Solid Films, 2006, 500, 336.

[2] I. Alekseeva, O. Dymshits, M. Tsenter & A. Zhilin, J. Non-Cryst. Solids, 2011, 357, 2209.

[3] M. A. Hughes, T. Suzuki & Y. Ohishi, Opt. Mater., 2009, 32, 368.

[4] J. Kong, D. Y. Tang, B. Zhao, J. Lu, K. Ueda, H. Yagi & T. Yanagitani, Appl. Phys. Lett., 2005, 86, 161116.

[5] Y. Lin, Y. Zhany, W. Huang, K. Lu & Y. Zhao, J. Non-Cryst. Solids, 1995, 112, 136.

[6] H. A. A. Sidek, I. T. Collier, R. N. Hamton, G. H. Saunders & B. Bridge, Phelos. Mag. 1989, 2, 221.

[7] M.M. El-Desoky & Shereif M. Abo-Naf, J. Mater. Sci., Mater. Electronics, 2004, 15,425.

[8] K. Błaszczak, W. Jelonek & A. Adamczyk, J. Molecular Structure, 1999), 511–512,163.

[9] Ch. SrinivasaRao, V. Ravikumar, T. Srikumar, Y. Gandhi & N. Veeraiah, J. Non-Cryst. Solids, 2011, 357, 3094.

[10] M. Y. Hassaan, F. M. Ebrahim, A. G. Mostafa & M. M. El-Desoky, Materials Chemistry and Physics, 2011, 129, 380.

[11] M. M. El-Desoky, F. A. Ibrahim & M. Y. Hassaan, Solid State Sciences, 2011, 13, 1616.

[12] M. Y. Hassaan, M. M. El-Desoky, M. G. Moustafa, Y. Iida, S. Kubuki & T. Nishida, Croat. Chem. Acta, 2015, 88 (4), 505.

[13] T. Nishida, J. Non-Cryst. Solids, 1994, 177, 257.

[14] G. K. Williamson & W. H. Hall, ActaMetallurgica, 1953, 1, 22.

[15] T. Nishida, J. Radioanal. Nucl. Chem., 1994, 182, 451.

[16] E. I. Kamitsus, M. A. Karakassides & G. D. Chryssikos, Phys. Chem. Glasses, 1986, 90, 4528.

[17] A. Burns, H. P. Brack & W. M. J. Risen, J. Non-Cryst. Solids, 1991, 131-133, 994.

[18] S. A. MacDonald, C. R. Schardt, D. J. Masiello & J.H. Simmons, J. Non-Cryst. Solids, 2000, 275, 72.

[19] H. Hirashima, D. Arai & T. Yoshida, J. Am. Ceram. Soc., 1985, 68, 486.

[20] R. Iordanora, Y. Dimitrieve, V. Dimitrov & D. Klissurski, J. Non-Cryst. Solids, 1994, 167, 74.

[21] M. Y. Hassaan, S. A. El-Badry, M. Tokunaga & T. Nishida, Croat. Materials Letters, 2005, 59, 3788.

[22] Safeya Ibrahim & Morsi M. Morsi, Materials Chemistry and Physics, 2013, 138, 628.

[23] Y. Gandhi, N. Venkatramaiah, V. Ravikumar & N. Veeraiah, Physica B: Condensed Matter, 2009, 404, 1450.

[24] S. Rada, L. Rus, M. Rada, E. Culea, N. Aldea, S. Stan, R. C. Suciu & A. Bot, Solid State Ionics, 2015, 274, 111.

[25] O. Tolstova, S. Stefanovsky & T. Lashtchenova, roceedings of the 2nd Balkan Conference on Glass Science and Technol, 14th Conference of Glass and Ceramics, Varna, 24-28 Sept. 2002.

[26] M. Y. Hassaan, S. M. Salem & M. G. Moustafa, J. Non-Cryst. Solids, 2014,391 6.

[27] E. A. Hayri & M. Greenblatt, J. Non-Cryst. Solids, 1987, 94,387

[28] L. Murawski, C. H. Chung & J. D. Mackenzie, J. Non-Cryst. Solids, 1979, 32, 91.

[29] M. Sayer, A. Mansingh, "Non-Crystalline Semiconductors", Vol. III, M. Pollak (Ed.), CRC Press, Boca Raton, FL, USA, 1987.

[30] M. Y. Hassaan, M. M. El-Desoky, S. M. Salem & S. H. Salah, J. Radioanal. NuclearChemistry, 2001, 249, (3) 595.

[31] M. M. El- Desoky, J. Non-Cryst. Solids, 2005, 351, 3139.